Journal of Marine Research, 71, 109–132, 2013

Numerical Study of Cold Dome Variability induced by Typhoon Morakot (2009) off Northeastern Taiwan

by Yaling Tsai[1], Ching-Sheng Chern[1,2], Sen Jan[1,3] and Joe Wang[1]

ABSTRACT

The ocean response to the passage of Typhoon Morakot (2009) near the continental shelf of the East China Sea off northeastern Taiwan was evaluated using a numerical ocean model to clarify how the permanent upwelling feature in this region was changed during this storm event. Several studies have identified the presence of the Kuroshio subsurface water in this Cold Dome region, which results from the interactions among the monsoon, the Kuroshio and the shelf topography. This study shows how tropical cyclone Morakot's passage quickly disturbed the circulation around Taiwan and induced a short-period intrusion of the Kuroshio water onto the continental shelf. The intrusion began during the second half of the forced period and lasted for approximately two days. The upwelling and northward flow were greatly enhanced during this period, allowing the subsurface water from the upstream Kuroshio to be transported onto the shelf and to reach the Cold Dome. The intrusion-induced cold anomaly along the north coast of Taiwan was much more significant than what can be achieved by local vertical mixing. The cold anomaly later formed an eddy, which gradually propagated with the Kuroshio to the northeast.

1. Introduction

The Kuroshio, offshore of northeastern Taiwan, changes its direction from northward to northeastward as it encounters the continental slope of the southern East China Sea (ECS). The turning of the Kuroshio is accompanied by a strong upwelling of cold and saline subsurface water intruding onto the shelf of the southern ECS (Hsueh et al., 1993). A counter-clockwise circulation pattern centered at (25.6°N, 122.1°E) is thus present as a persistent feature in this region (Jan et al., 2011). This Cold Dome region is affected by both the Kuroshio and the flow pattern of the surrounding seas, which are largely controlled by variations in the wind field of East Asia.

A typical time scale for the wind associated with the Cold Dome variability ranges from seasonal monsoon changes to short-term typhoon impulses. Both the northeasterly monsoon and typhoon can strengthen the intrusion of the Kuroshio onto the ECS shelf (Hsueh et al.,

1. Institute of Oceanography, National Taiwan University, P. O. Box 23-13, Taipei 106, Taiwan, R.O.C.
2. Corresponding author ***e-mail: cschern@ntu.edu.tw***
3. Taiwan Ocean Research Institute, National Applied Research Laboratories, Taiwan.

1992, Tsai et al., 2008a), but their response times are very different. The intrusion induced by the northeasterly wind occurs approximately a month after the onset of the winter monsoon season, and the intrusion due to a typhoon occurs within the wind-forced period (Chuang and Liang, 1994). Chang et al. (2010) demonstrated that upwelling along the northern shelf of Taiwan during northeasterly winds is created by the divergence and convergence produced by wind acting on the vorticity fields of two strong jets: the Kuroshio and the Taiwan Warm Current. Chern and Wang (1992a) also showed that the flow pattern off northern Taiwan depends on the dynamic balance between the Kuroshio and the Taiwan Strait outflows. However, there is not much literature reporting on how strong typhoon winds modulate the Kuroshio off northeast Taiwan and the associated post-storm variations on the flow field in that region.

In this paper, a three-dimensional primitive equation model is used to study the dynamic process of the upper ocean response to Typhoon Morakot (2009). Morakot was a category-2 typhoon and moved steadily westward along 23°N until it landed in Taiwan on Aug. 7, 2009. This typhoon produced record-breaking rainfall in Taiwan and caused severe damage. Specifically, we narrowed our focus to the dynamic response induced by the typhoon winds. The impacts of the large amount of rainfall on the regional circulation are significant and can be found in other relevant studies (Jan et al., 2013).

2. Typhoon case and model description

Based on data from the Regional Specialized Meteorological Center (RSMC) Tokyo - Typhoon Center, Typhoon Morakot formed as a tropical storm in the western Pacific near 134°E and 20°N on Aug. 3, 2009 (Fig. 1a). The storm moved northeastward for a day before it turned westward; it then continued in this zonal direction until it reached Taiwan on Aug. 7. Its intensity increased to that of a severe tropical storm on the Aug. 5 and to that of a typhoon on the Aug. 6. Morakot's translation speed slowed down as it achieved its maximum intensity later that day (Fig. 1b) with central pressure dropping to 945 hPa, which was maintained for approximately 24 hours. It then moved slowly towards Taiwan with decreasing wind speed and made landfall on central Taiwan at approximately 23Z on Aug. 7. Morakot's intensity decreased to that of a severe tropical storm after Aug. 8, and it moved into the Taiwan Strait later that day, with its path shifting to a northwestward direction. As it crossed 120°E in the Taiwan Strait, the storm turned again and headed northward, eventually making a second landfall in the Fu-Jian province of China.

Morakot's track falls into one of the prevailing paths of typhoons passing through Taiwan. According to the Central Weather Bureau of Taiwan, approximately 13% of the typhoons invading Taiwan from 1911 to 2010 follow this type of track. Tsai et al. (2008a) have shown that the daily summertime sea surface temperature (SST) data near the Cold Dome region in 2004∼2006 often decreased during storm events around Taiwan. There are approximately six types of tracks for these storm events. Among these types, the events resulting from the prevailing tracks almost always induce cooling of various degrees. Although it is affected by the storm intensity, sometimes the cooling magnitude is so significant (e.g. Chang et al., 2008) that it may have resulted from a Kuroshio intrusion event, as suggested

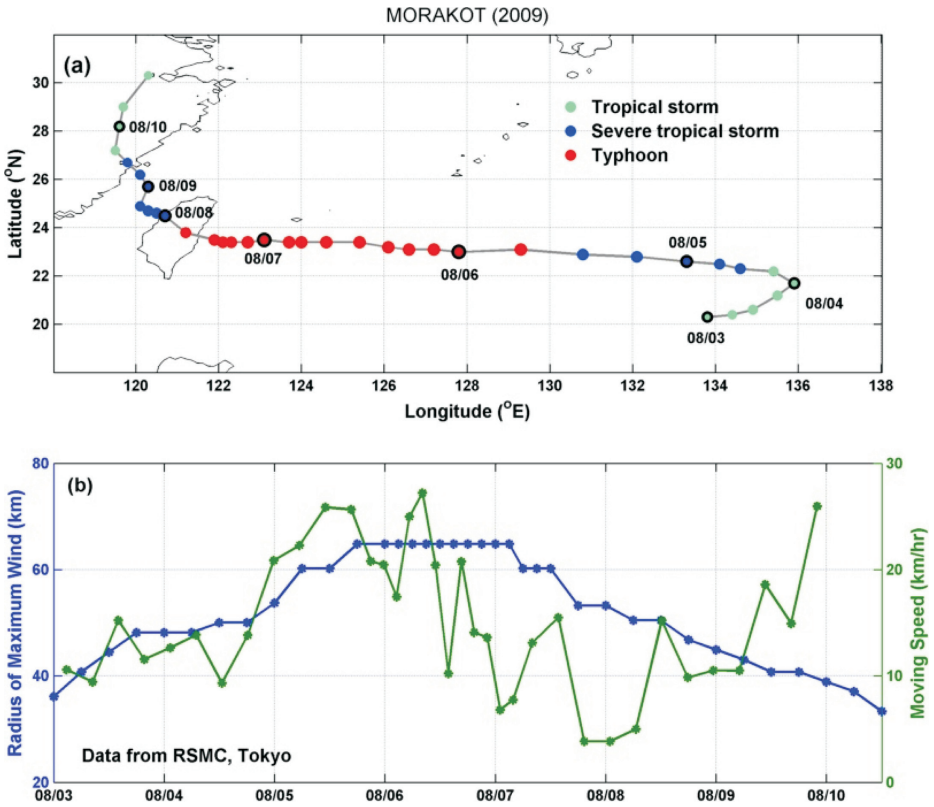

Figure 1. Track (a) and radius of maximum wind (b) for Morakot based on the best track data from the RSMC Tokyo. Morakot's moving speeds derived from them are also shown in (b).

by previous analyses of hydrographic data. During the Morakot event, Kuroshio subsurface water characteristics were also observed by the mooring arrays on the continental slope of the ECS (Gawarkiewicz et al., 2011). This model study aimed to provide auxiliary dynamic information for data obtained in the field experiment during the Morakot event.

The ocean model used is a z-level primitive equation model modified from Semtner and Mintz's study (1977). The model contains rigid-lid, hydrostatic and Boussinesq approximations and uses the level-2 turbulence closure scheme of Mellor and Durbin (1975) to estimate the vertical eddy viscosity. The model domain covers most of the northern Pacific (100°E ~ 120°W, 0~40°N) and the South China Sea, with a grid resolution of 0.2°. There are 25 vertical layers in the model, starting from the surface: the upper 250 m include eight layers at 12.5 m intervals and six layers in 25 m intervals; the next 250 m are divided into three layers at 50 m intervals and one 100 m layer; the next 3,500 m contain four layers at 125 m intervals and three layers at 1,000 m intervals. The maximum depth of the model is thus limited to 4 km. The model topography to the west of 150°E was established using

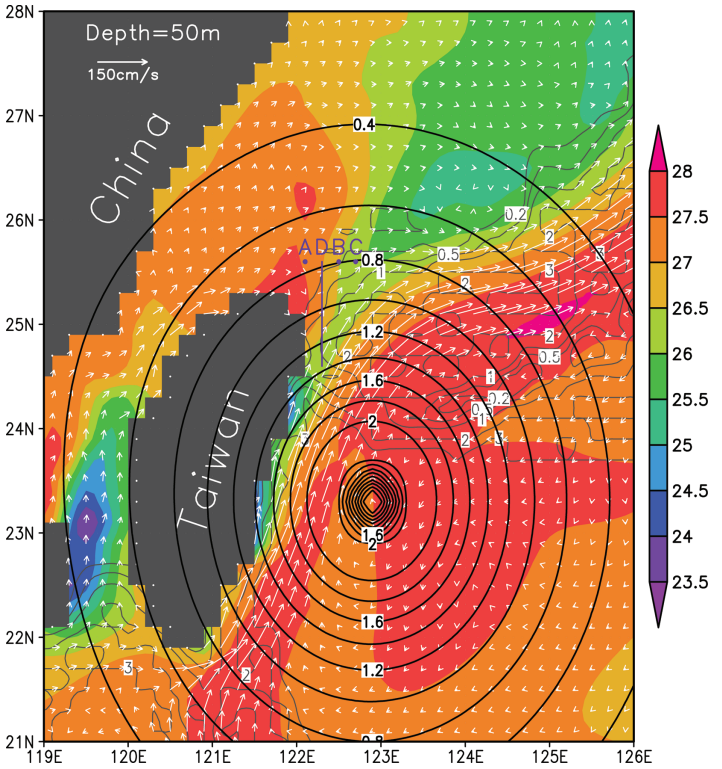

Figure 2. Model used initial temperature field (shaded contour, °C) and current vectors at 50 m depth in the region around Taiwan. The black contours show the model used wind stress (Pa) at 00Z, Aug. 07. The 0.2, 0.5, 1, 2, 3 (gray contour, km) isobaths are also superimposed. Note that the locations of the sites in Figure 11a-c are marked as A, B and C, respectively, and the location of the transect in Figure 9 is marked as D.

the five-minute depth database from ETOPO5 (National Geophysical Data Center 2001). The salinity in the model was held constant (35 PSU) throughout the entire calculation. The model was driven by applying annual mean wind stress and SST and integrated over three years, and then the forcing was changed to monthly mean wind stresses and SST and integrated for an additional three years. A model-produced quasi-steady state for August was thus generated and adopted as the initial field for this study (Fig. 2). Detailed model configurations are reported by Chern et al. (2010).

The typhoon winds used in the model were calculated based on the Rankine Vortex storm wind field, as follows (Holland, 1980):

$$-\frac{V^2}{r} - fV = -\frac{1}{\rho_0}\frac{\partial p}{\partial r},$$

where V is the wind speed; r is the distance to the storm center; f is the Coriolis parameter; ρ_0 is the air density; and p is the pressure. The pressure field of the storm was calculated as follows (Schloemer, 1954):

$$P(r) = P_c + (P_n - P_c) \exp\left[-\left(\frac{R_{mw}}{r}\right)\right],$$

where R_{mw} is the storm's radius of maximum winds; P_c is the storm central pressure; and P_n is the environmental pressure. The storm parameters, P_c and R_{mw}, were obtained from the Morakot's best-track data provided by the RSMC, and the resulted storm wind field was a symmetric wind field (Fig. 2). The storm's intensity and size were assumed to be constant during the six-hour best-track data interval, but the location of its center was interpolated linearly by time steps between its two issued positions.

The model's initial flow field around Taiwan is shown in Figure 2, in which the Kuroshio flows along the east coast of Taiwan and turns northeastward when it encounters the continental shelf of the ECS. The features of the Kuroshio in this region, such as its horizontal and vertical extension, velocity scale and the velocity core location, are all consistent with previous observations (Rudnick et al., 2011). The cold upwelling region off northeast Taiwan has also been reproduced. The Taiwan Strait outflow flows northward into the ECS, while one branch follows the north coast of Taiwan and joins the Kuroshio northeast of Taiwan.

Based on this initial condition, the model was integrated using a baroclinic time step of 150 seconds for 15 days with the storm wind field superimposed. The model-calculated ocean responses were output every five minutes and were processed into hourly data for the following analysis and plotting. Their differences from the initial field are referred to as the anomaly fields generated by the storm wind in this study.

3. Results

With the strong boundary current and the large variations in this region's topography, the strong winds of Morakot, whose track cut transversely across the Kuroshio east of Taiwan, would inevitably induce complicated responses in the seas around Taiwan. The model results will be presented separately, depending on whether or not the model typhoon was over the Kuroshio east of Taiwan. The forced stage refers to the time when the rotating typhoon wind is in effect, and the time after that is the relaxation stage. We further divide the forced stage into two periods, the passage of the front half and the rear half of the storm, in which the wind directions are either opposite or identical to the northward-flowing Kuroshio, respectively. The model results for the relaxation period are also discussed to illustrate the post-storm restoration of the ocean environment near the Cold Dome region.

a. The front half of the forced stage

Figure 3 shows the temperature and flow anomaly fields in the upper ocean around Taiwan every four hours from 15Z on Aug. 6 to 11Z on Aug. 7. During this period, the center of

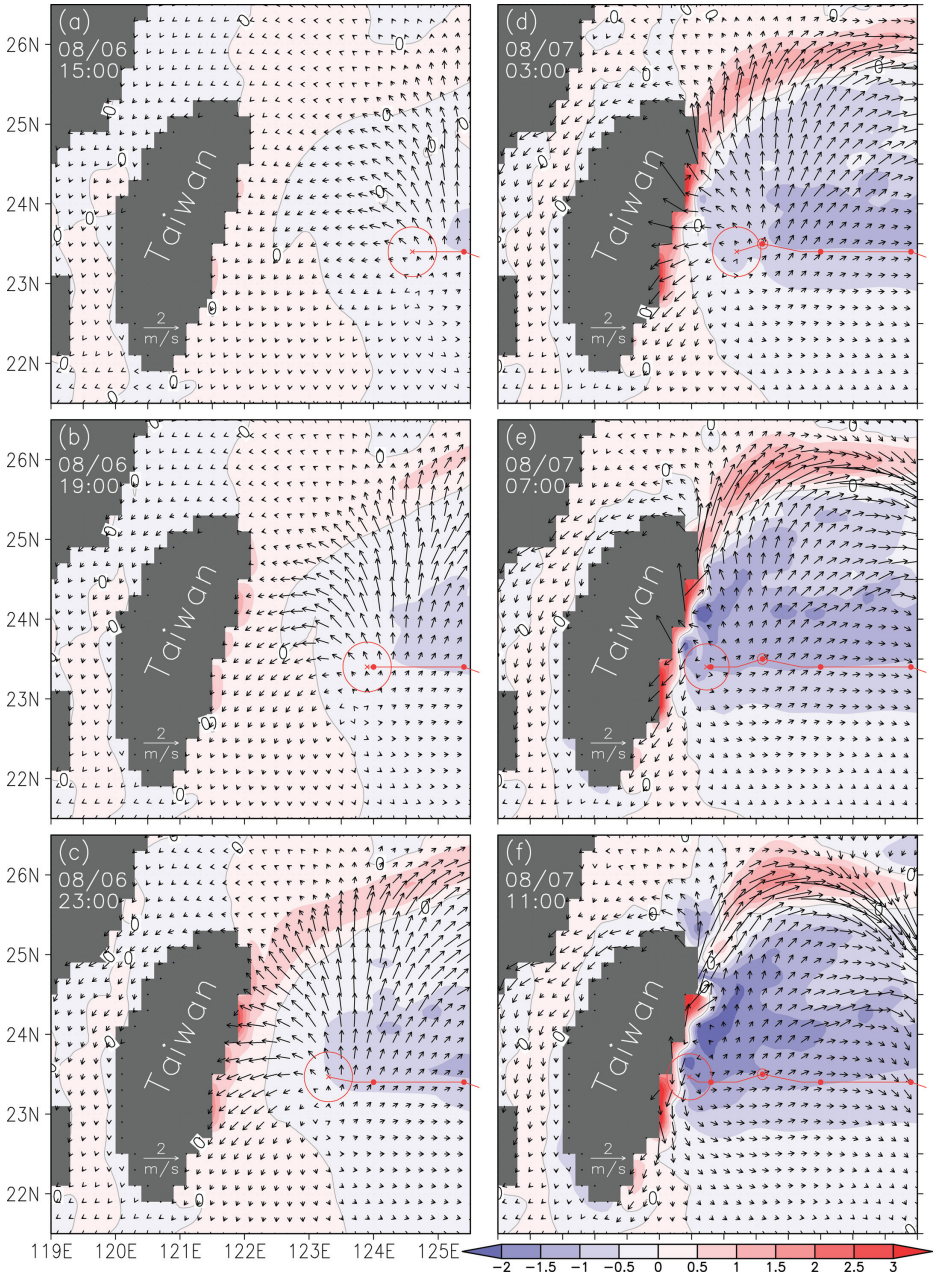

Figure 3. Snapshot of model-calculated temperature (shaded contour, °C) and flow (vectors) anomaly fields averaged over 0∼100 m or bottom depth during Morakot's front-half forced period for the Kuroshio flow region east of Taiwan. The red line is the storm track, and the gray areas represent the land above 50 m depth.

Morakot moved westward from approximately 124.5°E to 122°E along 23.4°N. The storm's intensity and speed both slightly decreased as it moved closer to Taiwan. Each plot in Figure 3 represents the model results averaged over 0∼100 m, or bottom depth, to illustrate the motions of the upper ocean induced by the wind.

The winds over the Kuroshio region were primarily northerly winds in the beginning of this period. With the approach of the storm, the wind speed increased and shifted with increasing eastward and westward components in the south and north of the storm center, respectively. However, the predominant feature of the anomaly field was the wind curl-induced divergent currents, which emanated from the storm center, but greatly intensified on the right-hand-side of the track (Figs. 3a-b). There was certainly a convergent zone formed outside of the divergent region, with its position determined by the wind field; nevertheless, the convergent zone in this case was eventually modified by the Kuroshio and the topography of this region as the storm kept moving west. When Morakot moved close to Taiwan, the divergent flow from the storm center converged to the east coast of Taiwan and the Kuroshio along the continental shelf of the ECS. The convergence caused downwelling near the land boundary, and ocean warming appeared along the shelf line with a maximum anomaly of approximately 2°C (Figs. 3c-e). The horizontal flow anomaly in the Kuroshio region east of Taiwan before the storm's arrival was primarily in the direction transversal to the Kuroshio. The current near the surface was flowing shoreward and converged at the coast, which then generated downward motion and a seaward return flow in the layer below 70 m. On the other hand, the flow anomaly in the shelf region followed the wind direction relatively closely because the water is shallow. The flow within the Taiwan Strait and on the shelf north of Taiwan therefore exhibited southwestward and westward anomalies, respectively (Fig. 3c-d). In another words, the Taiwan Strait outflow, which joined the Kuroshio off northeastern Taiwan, was slowed down.

When the storm center crossed the Kuroshio, the divergent flows east of Taiwan became aligned with the Kuroshio and caused positive and negative flow anomalies north and south of the storm track, respectively (Figs. 3e-f). The cooling trend north of the track became evident and extended downstream in the Kuroshio flow region. In the meantime, the flow anomaly on the ECS shelf along the northern coast of Taiwan and in the Taiwan Strait grew with time due to the northeasterly wind associated with the storm's front half (Figs. 3e-f). Near the northeastern tip of Taiwan, the flow anomaly rotated to the northeast with an enhanced northward component. This region became a significant divergent zone, and upwelling appeared in the lower layer to replace the water that had diverged in the surface layer. It was at this time that the cooling off northeastern Taiwan was first observed in the model (Figs. 3e-f).

b. The rear half of the forced period

During the second half of the forced period, Morakot made landfall on Taiwan's east coast and headed northwest across Taiwan, entering the Taiwan Strait (Fig. 4). Morakot

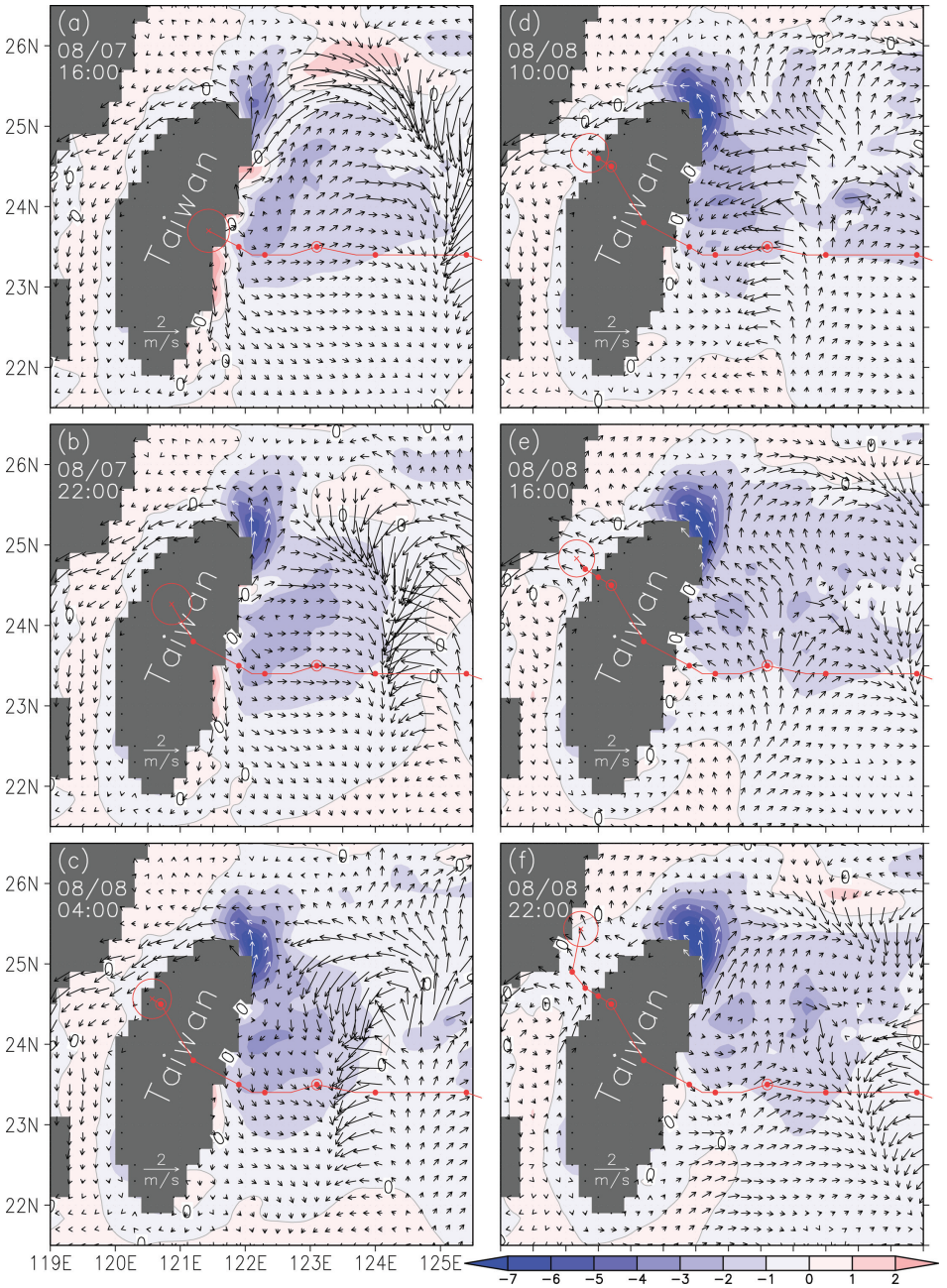

Figure 4. Same as Figure 3, but for the rear-half forced period.

was reduced to a smaller severe tropical storm after landfall. The wind forcing in the Kuroshio region was no longer a northerly wind, but changed to an intense southerly wind. The near-inertial motion became dominant to the east of Taiwan, and the ocean temperature decreased due to the storm-induced upwelling during this period. From Figures 4a-b, we can infer that the upwelled cold water was further transported downstream by the Kuroshio towards the continental slope region off northeast Taiwan. Hence, the warming along the shelf break of the southern ECS generated in the previous period was gradually replaced by cooling. Further east, the cooling was more significant north of the track and fluctuated with the inertial motion; its peak value was approximately -4°C at 24°N (Figs. 4c-d).

In the Taiwan Strait, the southward along-strait flow anomaly continued to grow as the storm was crossing Taiwan (Figs. 4a-c). Hence, the cold anomaly continued to develop during this period as the intrusion process off northeastern Taiwan persisted. The cold water spread outward from this region with enhanced northward and westward flows and eventually covered a round area spanning one degree in latitude and longitude, centered southwest of the Cold Dome area (Fig. 4f). As Morakot moved into the Taiwan Strait, the cross-strait flow component gradually increased (Figs. 4d-f). The flow anomalies in the strait were influenced by the northwestward shifting of the storm track and gradually turned northward in the southern strait, particularly along Taiwan's west coast (Figs. 4e-f). In the northern strait, the flow anomaly was weaker, but was still moving west during this period, so the upwelling near the Cold Dome area continued. The cold-water intrusion process persisted for over 24 hours and resulted in a significant cooling of approximately -7°C below a depth of 50 m (Fig. 4e).

c. Relaxation period

As Morakot made landfall in China's Fu-Jian province, the Kuroshio flow region was out of the direct influence of the storm wind. To examine how the ocean in this region was restored to its pre-storm condition, we adopted a time average over a local inertial period (IP) to remove the inertial motion from the model results and plotted the upper 100 m mean temperature anomaly and horizontal flow in Figure 5.

The flow in the Taiwan Strait reverted to pre-storm direction after Aug. 9 with the aid of Morakot's northward movement after entering the strait. The northern Taiwan Strait and the southwestern ECS were still affected by the storm wind within the averaging IP shown in Figure 5a; as such, there was a strong northward flow emanating from the Taiwan Strait. Originally, this outflow should have flowed along Taiwan's north coast to join the Kuroshio, but in this case, it was blocked by the cold anomaly off northeastern Taiwan. Therefore, it primarily turned eastward after passing over the cold anomaly area (Figs. 5a, d). The outflow restoration weakened the divergence off northeastern Taiwan, and both northward and westward expansion of the cold anomaly ceased. The northward intrusion of the Kuroshio still confined the east edge of the cold anomaly to the west of 122.5°E.

The strength of the cold anomaly was reduced with time. Meanwhile, cyclonic circulation gradually began to form over the study region, and the westward span of the cold anomaly

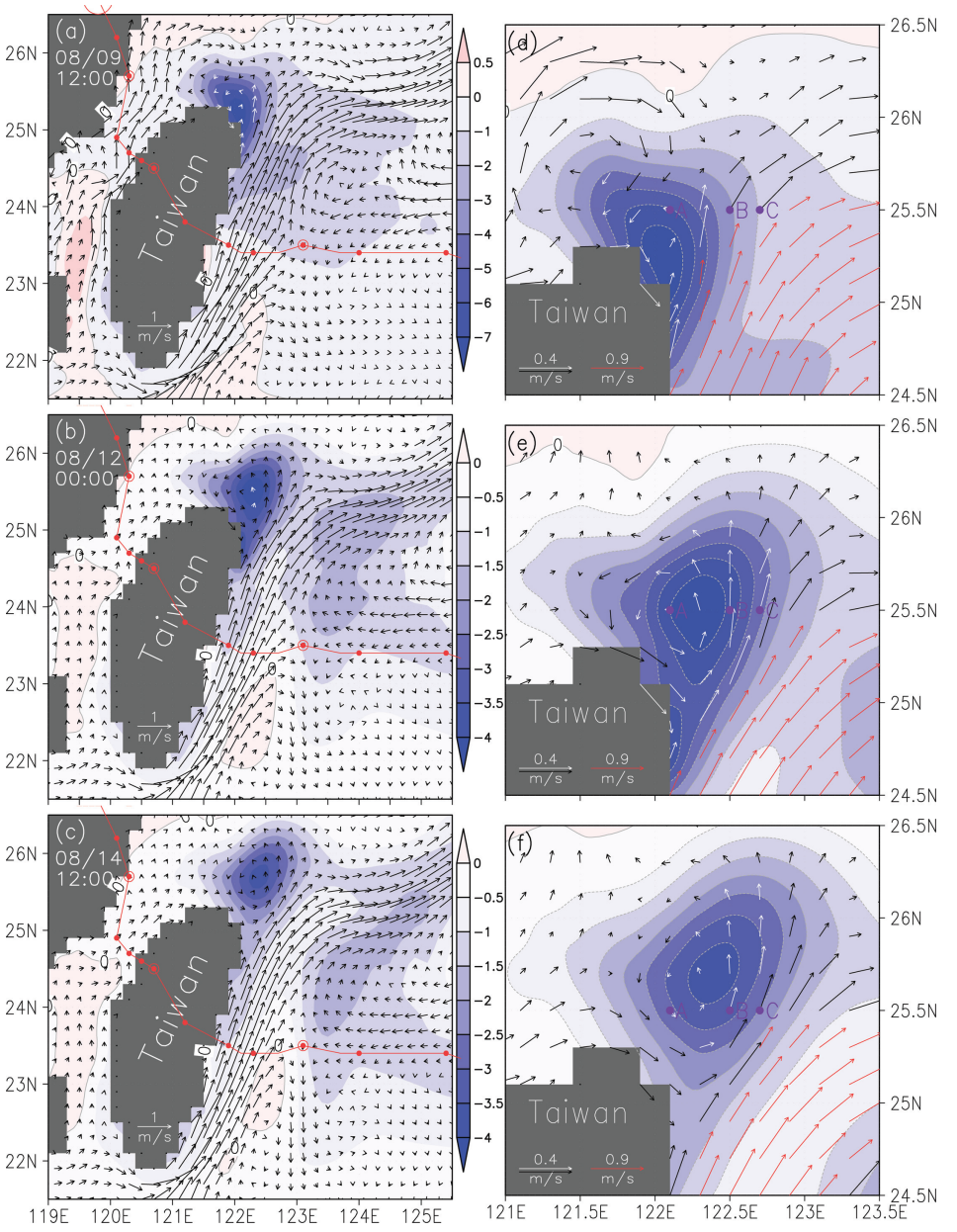

Figure 5. (a-c) Model-calculated, upper 100 m mean temperature anomaly (shaded contour) and flow (vectors) averaged over one inertial period (1 IP = 28 hours) during Morakot's relaxation period. The storm track (red line) is superimposed. The flow near the cold anomaly region in (a-c) was enlarged in (d-f). Note the labels A, B, and C denote the location of the sites in Figure 11.

retreated as the intrusion process weakened (Figs. 5b-c). The relatively warmer Taiwan Strait outflow along the north coast of Taiwan cut through the cold anomaly, causing the anomaly contours to become closed around the Cold Dome region and then form into a cold eddy (Figs. 5e-f). As the Kuroshio shifted to its original position, the cold eddy's axis gradually aligned with the Kuroshio flow direction and drifted northeastward (Figs. 5b-c). The cold eddy presumably propagated with the velocity of the Kuroshio's western edge and is estimated to have been approximately 12 cm/s. This propagation speed is close to the drifting speed of a freshwater pulse observed in this region during the Morakot event (Jan et al., 2013).

d. Budget analysis of temperature and vorticity at the Cold Dome area

In the open ocean, typhoon-induced cooling was primarily caused by two processes. One is due to the Ekman pumping associated with the wind stress curl from a slow moving storm (less than 3 m/s), and this cooling occurs along the storm track. The other is due to the enhanced mixing that occurs 0.5–1 degrees of latitude to the right of the storm track when nearly inertial resonance between the typhoon wind and ocean response occurs (Tsai et al., 2008b). The Cold Dome site is relatively far away from the track of Morakot (Fig. 1) and still underwent strong cooling during the storm event. Therefore, it is important to know the dominant cooling process there. Figure 6a shows the time variations in the vertical profile of the total cooling rate (°C/day) at a site within the Cold Dome (Site A in Fig. 2). This cooling tendency is roughly equal to the sum of the advective heat flux gradients in the x-, y- and z-directions (Figs. 6b, c and d, respectively), while the contribution from the diffusion process is very small (Fig. 6e). This feature suggests that the cooling within the Cold Dome is primarily due to advective processes. We can further infer that the cooling occurring below a depth of 50 m is caused by divergence in the vertical heat flux (Fig. 6d), and the surface layer above 50 m forms a sink for the upwelled cold water, which must spread laterally out of the Cold Dome region. Figures 6b and 6c indicate that the upwelled water was primarily moved in the x-direction (i.e., the upwelled cold water was transported eastward in the shelf area).

In addition to the significant cold anomaly formed near the Cold Dome (Fig. 5), the intrusion event also changed the vorticity field in this region. The mean vorticity in this region was originally weakly positive, so there must have been a positive vorticity input during this event for a cold cyclonic eddy to form after the storm had passed. The wind curl was always negative near the Cold Dome because this region was out of the storm's radius of maximum wind. The vorticity analysis based on the model results indicates that the positive vorticity source was transported by the Kuroshio. Integrating the vorticity tendency term over a specified time interval for the average of the upper 100 m yielded the relative vorticity change in the Cold Dome region during the active intrusion period and one subsequent IP (Fig. 7). Figure 7 also shows the individual contribution to the vorticity change from the stretching of the planetary vortex tube and from the northward transport of

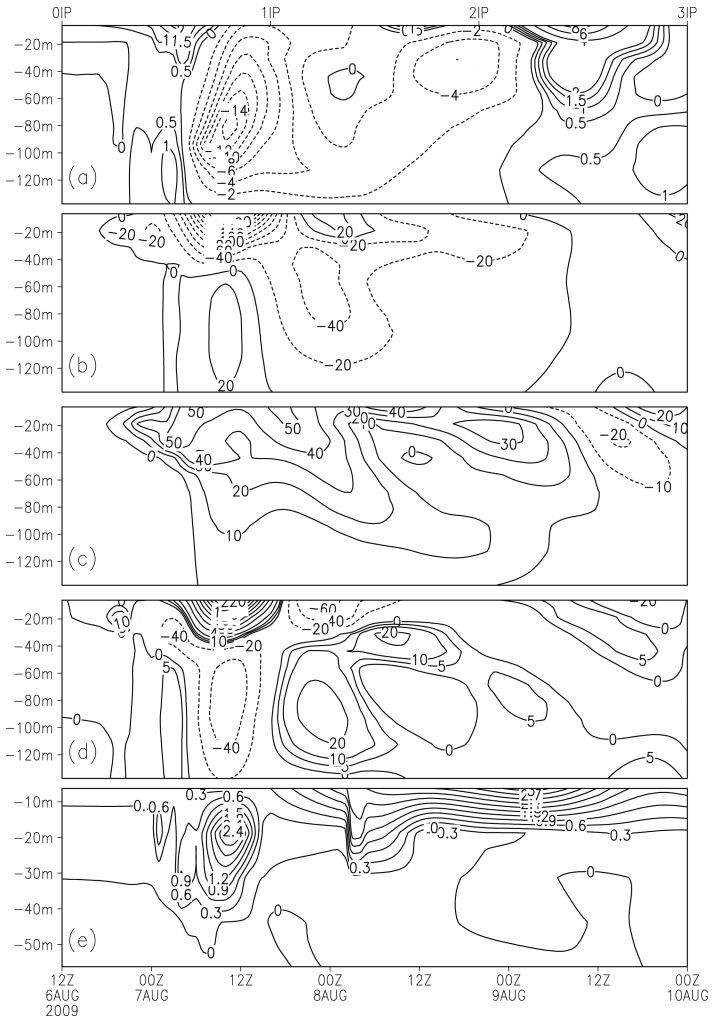

Figure 6. Time rate change of the model-calculated temperature (°C/day) profile at a site within the cold dome (a), the advective heat flux gradients in the x- (b), y- (c) and z-directions (d) and the vertical diffusive heat flux gradients (e) during the Morakot event. Note that the diffusive term (e) below 50 m depth was small and thus not shown. The IP scaling of the time frame was also added on the top.

the Kuroshio, as the mean flow during these two periods was northward. This observation demonstrates that during the active intrusion period, the water column was compressed by the upwelling motion when it moved onto the shelf, and the vorticity decreased. In the subsequent downwelling period, the process reversed, and its contribution became positive. On the other hand, the northward transport of the vorticity associated with the Kuroshio's

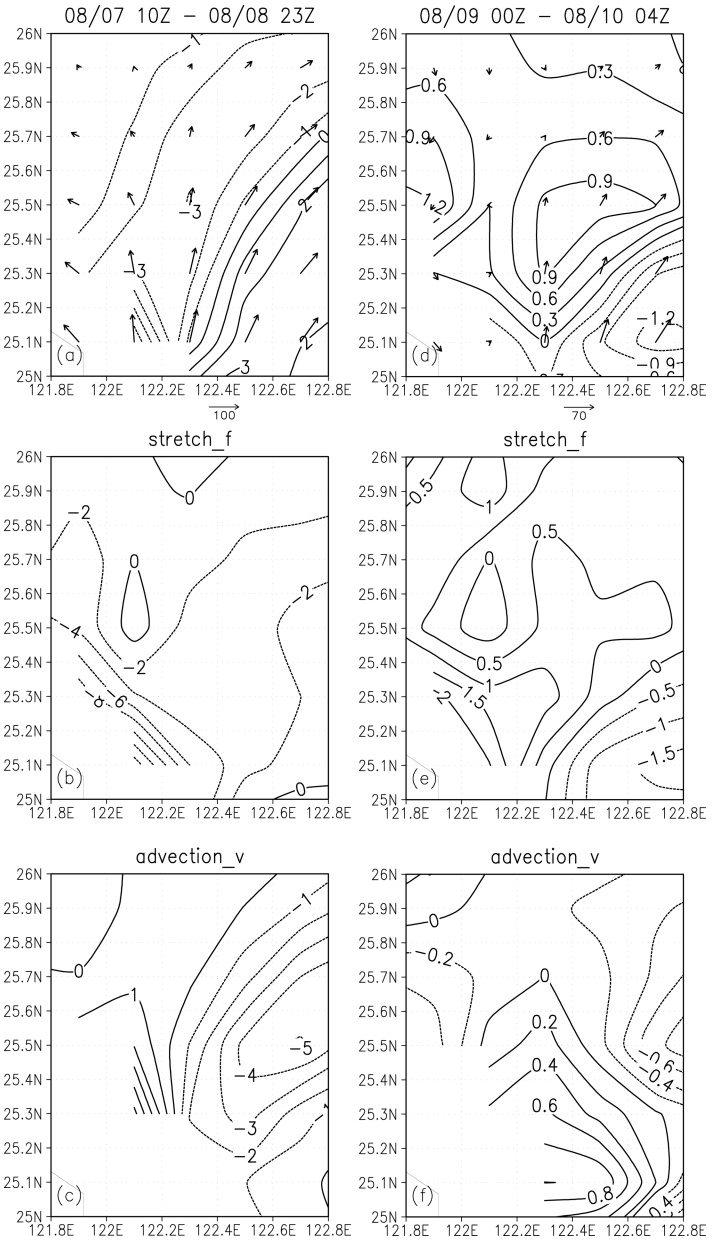

Figure 7. Upper 100 m averaged vorticity change ($\times 10^{-5}$ s^{-1}) within the active intrusion period (a) the contribution from the stretching of the planetary vortex tube (b) and the advection process in the y-direction (c) near the cold dome region. (d-f) are the same as (a-c), but for the period 1 IP after the active intrusion period. Both periods are specified on the top panel. Note that time-averaged upper 100 m mean current (cm/s) is also shown on the top panel.

western flank to this region remained positive throughout both periods. As a result, the mean vorticity was gradually increased during the relaxation period.

To gain insight into the dynamic role of the Kuroshio on the formation of the cyclonic circulation off northeastern Taiwan, we also ran a case with the same numerical settings, but the ocean was initially quiescent with vertical temperature stratification only. Figure 8 depicts the upper 100 m mean temperature anomaly and horizontal flow, after averaging over one local IP, of this new case at the same time as those in Figure 5. It clearly shows that there was no cyclonic eddy formation after the storm passage when the Kuroshio was not present in the model. The cold anomaly occurred mostly to the right of the track, and the residual flow off northeastern Taiwan was primarily to the west as a result of the storm-induced flow encountering the land and flowing along the coast. The northward spread of the cold anomaly did not appear in this case, nor did the cold eddy formation during the relaxation period. The cold anomaly to east of Taiwan persisted longer because there was no downstream transport by the Kuroshio.

4. Discussion

The model results previously described illustrate an example of how the storm-induced response in the region off northeastern Taiwan is rather complicated compared to the response in the open ocean. The root cause is the turning of the ECS shelf and the consequent collision of the Kuroshio coming from east of Taiwan. The responses specific to this region include enhanced downwelling warming due to the Kuroshio and the topography, cooling contributed by the intrusion of the Kuroshio's subsurface water, and formation of a cyclonic eddy during the relaxation period. Intrusion of Kuroshio water in this region is known to be more significant in winter than in summer. The corresponding mechanism for winter intrusion involves the Ekman transport-induced shoreward movement of the Kuroshio and the decreasing of the northward pressure gradient in the Taiwan Strait (Chern and Wang, 1992b). The storm-induced intrusion, on the other hand, is also believed to be aided by the increase in the eastward sea level gradient and the subsequent larger northward current in the Kuroshio (Morimoto et al., 2009). The resulting time scale to trigger the intrusion is much shorter than the winter event, which occurred approximately one month after the initiation of the northeastern monsoon (Chuang and Liang, 1994). In this study, the intrusion started when the study region entered the forced period for approximately one day and the on-shelf flow had lasted for approximately two days, which may have ended early as a result of the northward movement of the storm. Figure 9 shows the upwelling rate in the upper ocean of the meridional transect at 122.3°E during the Morakot event. It shows that the downwelling motion was evident in the front half of the wind period in the middle section of the transect where the continental shelf is located. The upwelling was first observed south of the transect, where the land boundary is further west and the wind-induced divergence was strong. A few hours later, the upwelling occurred in the middle and northern sections and was accompanied by the westward and then northward currents in the layer. The upwelling started first

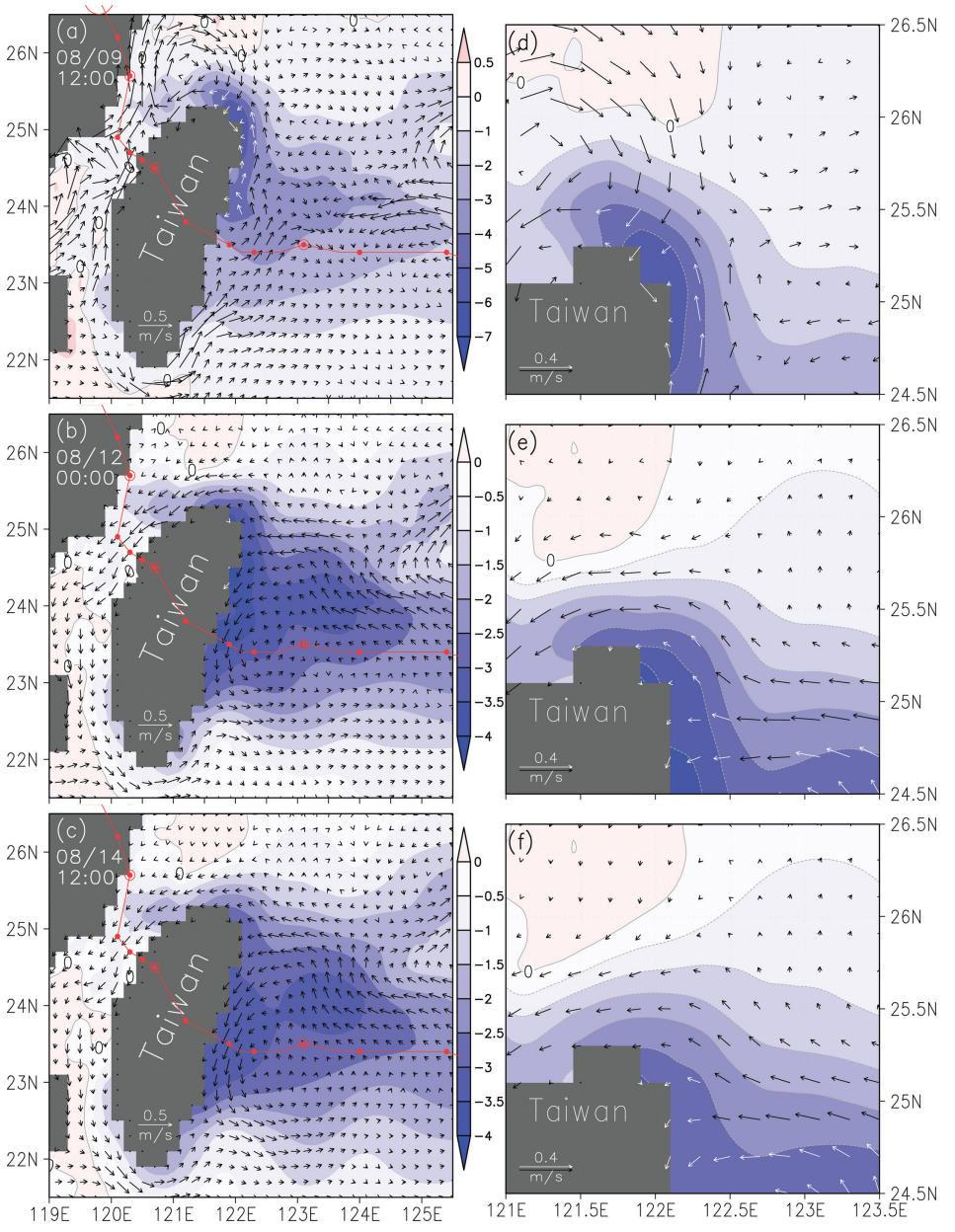

Figure 8. Same as Figure 5, but for the case of quiescent initial ocean conditions.

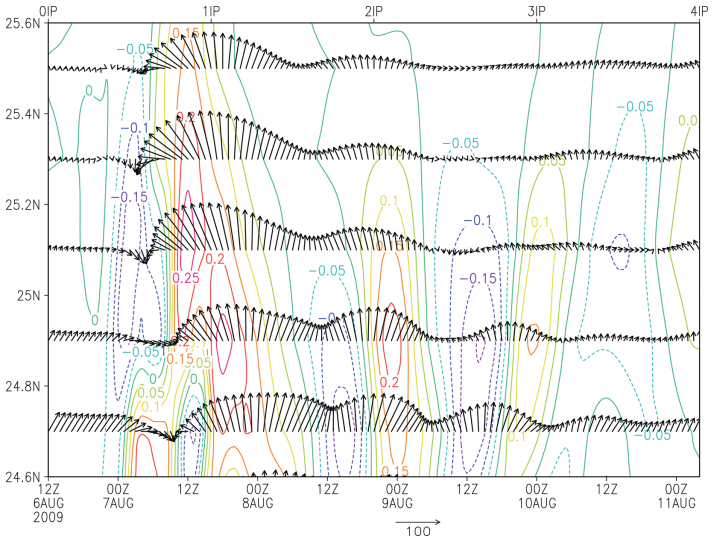

Figure 9. Time-latitude plot of the model-calculated vertical velocity and the horizontal current vector (north: upwards) averaged over the depth of 68–162 m during the Morakot event at 122.3°E. The velocity units are in cm/s. Note that the location of this transect is shown in Figure 2.

on the shelf and then extended southward, and the maximum value appeared near the slope at a rate of 0.25 cm/s at approximately 12∼16Z on Aug. 7 across the continental slope. The short period downwelling peak at 12Z in the south of the transect was due to the blocking of the shoreward flow by the land boundary. The upwelling decreased and stopped after Aug. 8, and inertial oscillations dominated for the remainder of the period. A larger northward flow component continued across the transect until Aug. 9, and no significant northward flow appeared on the shelf north of 25°N after approximately 06Z, at which time we infer that the intrusion event ended.

The storm-induced intrusion event was short, but intense, so it allowed the upstream Kuroshio subsurface water to enter the shelf and modify the hydrography of the Cold Dome region. Figure 10 shows the particle trajectory calculated from the model's hourly output, which traced a particle that arrived in the Cold Dome region at a depth of 50 m on August 9^{th} back to its original location. This analysis shows that the particle that intruded onto the shelf in the late forced period originated from the Kuroshio at a depth of approximately 180 m near I-Lan Ridge (122.4°E, 24.6°N) on Aug.6. The particle departing from there was first pushed downward, but still followed the normal path until approximately 06Z on Aug.7 when the vertical velocity became positive. The flow six hours later shifted to a northward direction with a large upwelling rate, and the particle was transported across the shelf break in one day's time and continued onto the shelf, reaching the Cold Dome in another half-day. The trajectory after Aug. 9 shows that the particle had inertial motion with a mean off-shelf downward displacement.

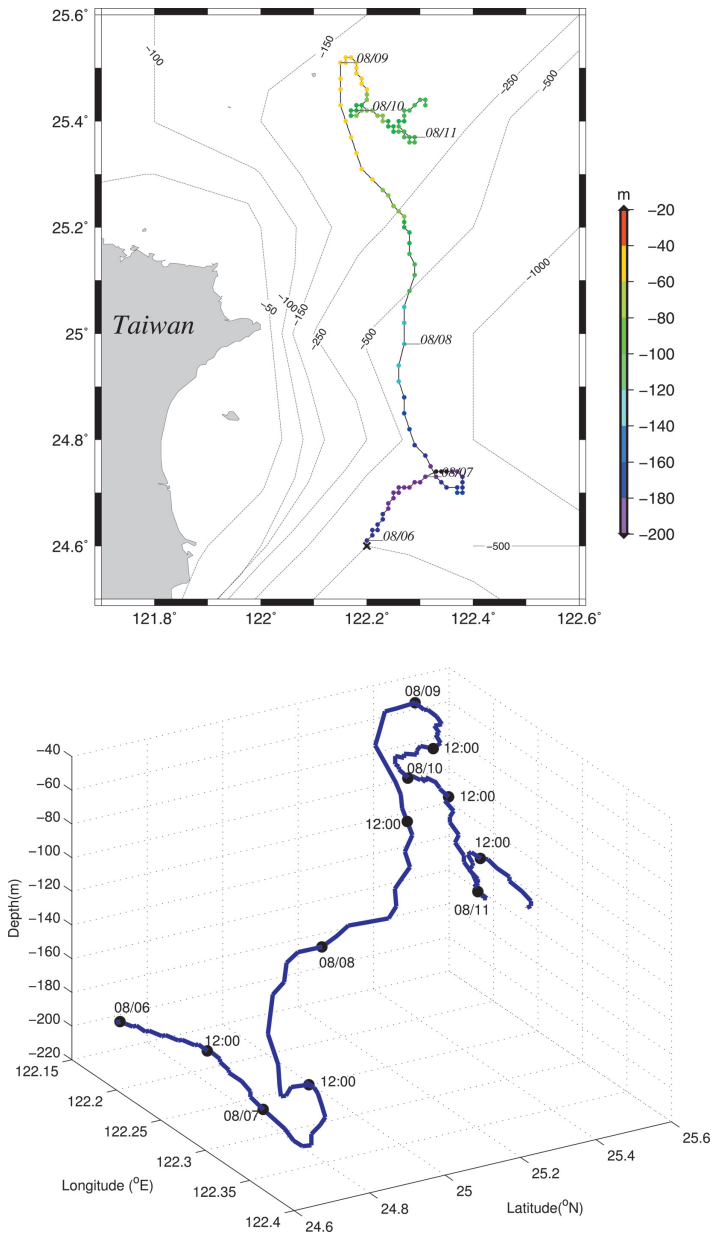

Figure 10. Trajectory plot (upper: two-dimensional; lower: three-dimensional) for the particle from the Kuroshio subsurface layer during the Morakot event. The depth contours (m) in the model are also shown in the two-dimensional plot.

a. Comparison with in situ measurements

Based on the data obtained from five moorings near the Cold Dome region and one site approximately one degree south of the Cold Dome, Gawarkiewicz et al.. (2011) showed the potential temperature and salinity plots from before (Aug. 6), immediately after (Aug. 11) and several days after (Aug. 15) Typhoon Morakot near the Cold Dome region. From that figure, it is evident that the water masses near the Cold Dome were modified from the slope-water type to the water type associated with the subsurface Kuroshio water after the Morakot event, and this observation is consistent with the trajectory plot shown in Figure 10.

The presence of the intruded upwelling water causes the storm-induced cooling to become more significant than the consequence of simple vertical mixing. Figure 11a shows the model-calculated temperature anomaly during the Morakot event at the Cold Dome. The temperature at the Cold Dome began decreasing when the storm was about to make land-fall on Taiwan (Fig. 11a). It continued decreasing and reached a minimum of -7°C on approximately Aug. 9 in the layer between 50$\sim$100 m. The bottom temperature at this site decreased from the initial value of 19°C to 17°C during this event, which indicates that cold water was transported here. Figure 4 of Jan et al. (2013) demonstrated that the coastal temperature (6 m below the sea surface) at the Peng-jia-yu Island station (Fig. 1 of Jan et al., 2013) decreased $\sim$6°C from Aug. 6 to Aug. 10. Our model calculated a -5°C cooling at 10 m depth during the Morakot event (Fig. 11a) at the Cold Dome region (near Peng-jia-yu), and this cooling magnitude is comparable to the observations.

The sea surface height anomaly (SSHA) figures covering the NE-offshore area during the Morakot event can be obtained from the AVISO web site (http://las.aviso.oceanobs.com/las/getUI.do). These figures show that the passage of Morakot induced a negative SSHA along the Kuroshio east of Taiwan. The sea surface height and the geostrophic currents in the region northeast of Taiwan before Aug. 6 and after Aug. 13 the impact of Morakot were also available from the NOAA web site (http://oceanwatch.pifsc.noaa.gov/las/servlets/dataset). These figures clearly show that the cyclonic feature in the Cold Dome region was enhanced after the storm's passage. As shown in Figure 12, the flow field derived from measurement is also consistent with our model results.

In addition to contributing to significant cooling, the intruding water also extended the cooling duration and masked the inertial oscillation signal in the temperature record. This effect can be observed in the model-calculated temperature anomaly during the Morakot event at two other sites east of the Cold Dome (Figs. 11b, c). Because these sites are closer to the continental slope, the downwelling-induced warming occurred first before the storm center arrived and in turn delayed the storm-induced cooling for several hours (Figs. 11b, c). The cooling, in comparison with that in the Cold Dome region, was weaker and had a more pronounced inertial oscillation. The temperature records from these two sites indicate that cooling was enhanced by approximately 1.5°C in the relaxation period at approximately 50 m depth after Aug. 10. From Figures 5e-f, we can infer that this further cooling was due to the arrival of the cold eddy, which detached from the north coast of Taiwan after the intrusion had stopped. Because the eddy was propagating to the northeast, the temperature

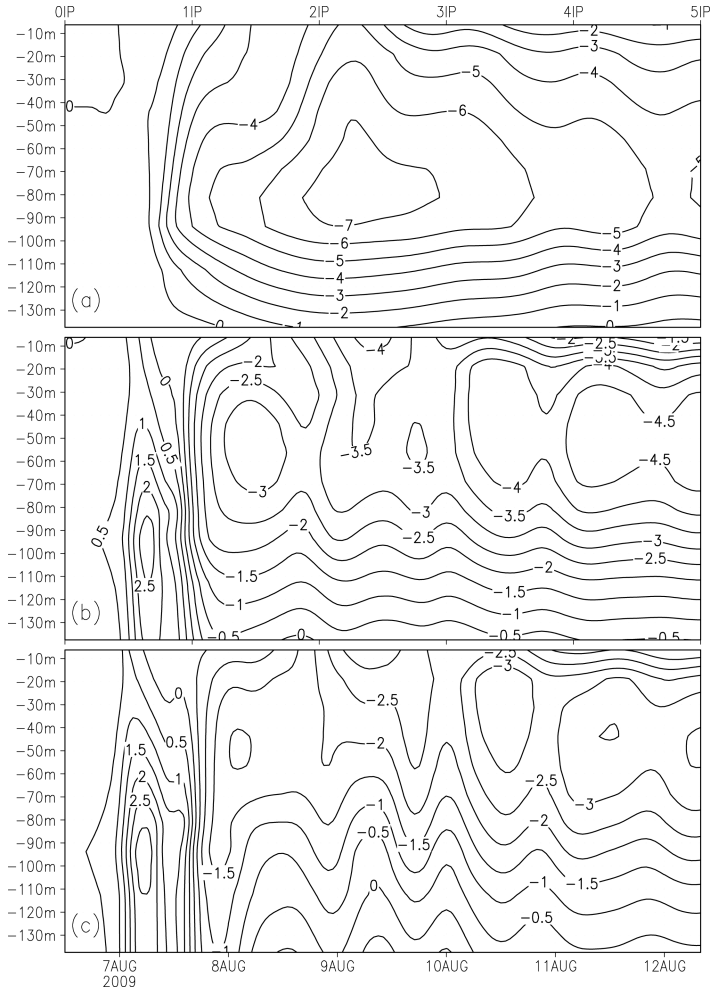

Figure 11. Time-depth plot of the model-calculated temperature anomaly (°C) at a latitude of 25.5°N and longitudes of 122.1°E (a), 122.5°E (b) and 122.7°E (c). Note that the locations of these sites are shown in Figures 2 and 5.

of the site to the east (Fig. 11c) was not affected by the core, but rather by the edge of the eddy, which resulted in a smaller cold anomaly than at the middle site. In this way, a particular temperature response to the storm passage in this region could signify significant cooling (Fig. 11a) or a delayed intensification of cooling (Figs. 11b-c). The hydrographic surveys occurring Aug. 13–17, 2009 in the area northeast offshore of Taiwan do indicate the presence of a cold anomaly extending northeastward from the Cold Dome site (Figs. 12–13 of Jan et al., 2013). The enhancing of the cold anomaly during the relaxation period can also

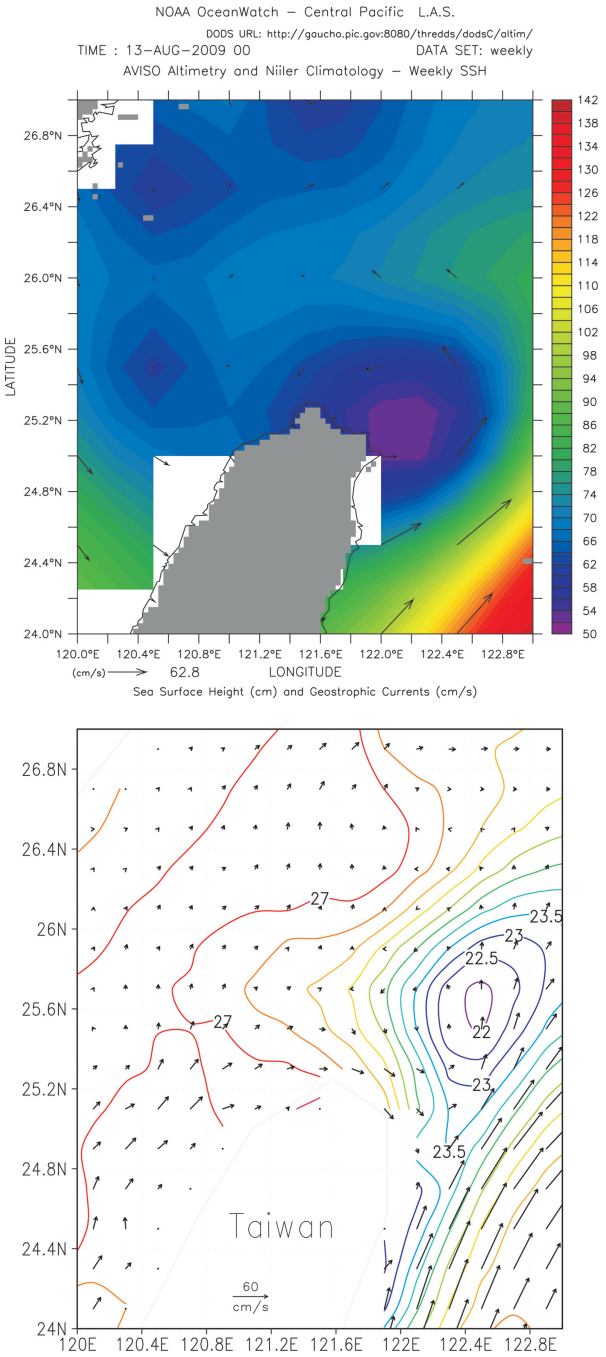

Figure 12. Sea surface height and geostrophic current vectors for Aug. 13, 2009 downloaded from the NOAA web site (upper). Model-calculated upper 100 m mean temperature (°C) and currents for the same region averaged over 1 IP centered at 00Z on Aug. 13 (lower).

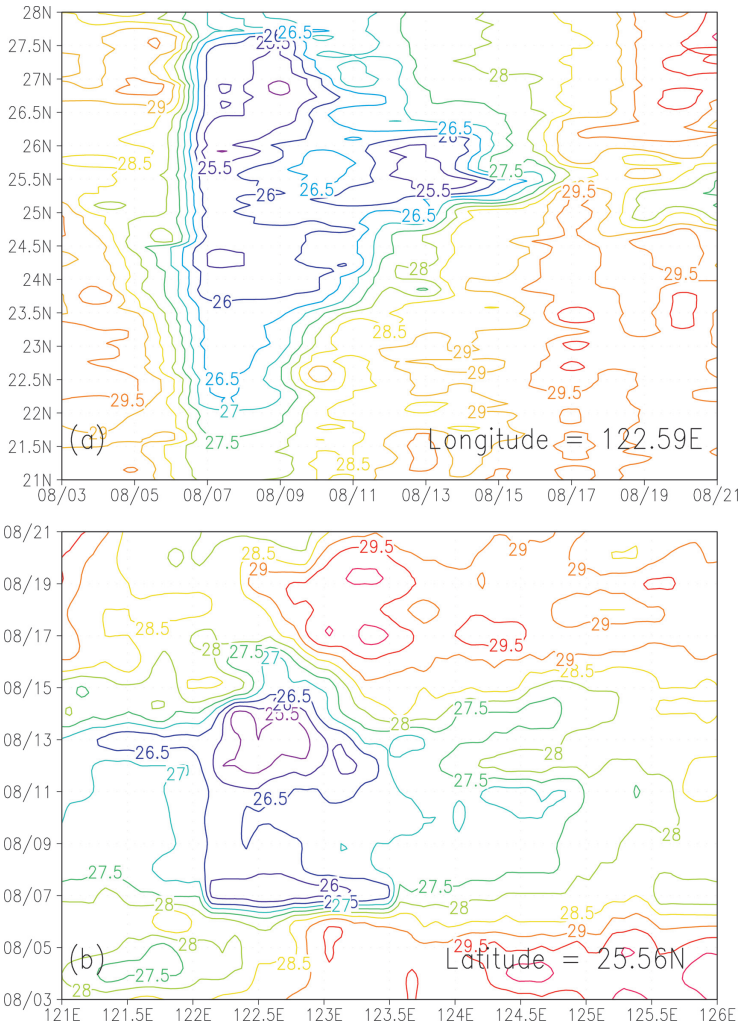

Figure 13. Time variation of the SST (°C) of two transects near the Cold Dome region during the Morakot event. Data was obtained from www.ssmi.com with resolutions of 9 km.

be found in the daily SST time series near the Cold Dome region obtained from the Remote Sensing System (www.ssmi.com) during the Morakot event. As shown in Figure 13a, the time latitude plot along the meridional transect at 122.59°E shows that the SST between 21°N and 28°N quickly dropped in the early forced period (Aug. 6). In the relaxation period, the SST gradually increased at all latitude except near 25.6°N where the SST decreased again for about 1°C at 08/13 (Fig. 13a). The SST data of the zonal transect at 25.56°N (Fig. 13b) shows that the cold anomaly enhanced in the relaxation period spreads from

122°E to 123°E and this is in agreement with our model results shown in Figure 5f. The cooling duration of the cold anomaly judged from the SST data extends for more than a week near the Cold Dome region and is consistent with the model result of the cold eddy formation and its following northeastward propagation.

5. Summary

This study investigated the variation in the upwelling region of the ECS's shelf off northeastern Taiwan during Typhoon Morakot (2009). The water mass in this region was known to be modified by the Kuroshio water brought onto the shelf through various mechanisms. We used a numerical ocean model to simulate how the regional circulation was altered by the storm wind, and the results show that the study area became a significant divergent zone during the passage of Morakot. Large upwelling and northward flow occurred and lasted for approximately two days. Upstream subsurface Kuroshio water was able to intrude onto the shelf and modify the temperature in the upwelling region. Significant cooling appeared along the northeast coast of Taiwan and extended outward with the intruding flow. After the intrusion process stopped, the cold anomaly gradually formed into a cold eddy and was drawn by the Kuroshio, propagating to the northeast.

Acknowledgments. This study was sponsored by a grant from the National Science Council of Taiwan, NSC 101-2611-M-002-011 and NSC 101-2811-M-002-160. Field data provided by the Quantifying, Predicting and Exploiting Uncertainty (QPE) experiment were consulted in the preparation of the manuscript.

REFERENCES

Chang, Y.; H.-T. Liao; M.-A. Lee; J.-W. Chan; W.-J. Shieh; K.-T. Lee; G.-H. Wang and Y.-C. Lan. 2008. Multisatellite observation on upwelling after the passage of Typhoon Hai-Tang in the southern East China Sea. Geophys. Res. Lett., *35*, L03612, doi:10.1029/2007GL032858.

Chang, Y.-L.; L. Y. Oey; C.-R. Wu and H.-F. Lu. 2010. Why are there upwellings on the northern shelf of Taiwan under northeasterly winds? J. Phys. Oceanogr., *40*, 1405–1417.

Chern, C.-S. and J. Wang. 1992a. The influence of Taiwan Strait waters on the circulation of the southern East China Sea. La mer, *30*, 223–228.

Chern, C.-S. and J. Wang. 1992b. On the seasonal variation of the Kuroshio intrusion onto the East China Sea. Acta Oceanographica Taiwanica, *29*, 1–17.

Chern, C.-S.; S. Jan and J. Wang. 2010. Numerical study of mean flow pattern in the South China Sea and the Luzon Strait. Ocean Dynamics, *60*, 1047–1059, doi:10.1007/s10236-010-0305-3.

Chuang, W.-S. and W. E. Liang. 1994. Seasonal variability of intrusion of the Kuroshio water across the continental shelf northeast of Taiwan. J. Oceanogr., *50*, 531–542.

Gawarkiewicz, G.; S. Jan; P. Lermusiaux; J. McClean; L. Centurioni; K. Taylor; B. Cornuelle; T. F. Duda; J. Wang; Y. J. Yang; T. Sanford; R.-C. Lien; C. Lee; M.-A. Lee; W. Leslie; P. J. Haley Jr.; P. P. Niiler; G. Gopalakrishnan; P. Vélez-Belchí; D.-K. Lee and Y. Y. Kim. 2011. Circulation and intrusions northeast of Taiwan: Chasing and predicting uncertainty in the Cold Dome. Oceanography, *24*, 4, 110–121.

Holland, G. J. 1980. An analytic model of the wind and pressure profiles in hurricanes. Mon. Wea. Rev., *108*, 1212–1218.

Hsueh, Y.; J. Wang and C.-S. Chern. 1992. The intrusion of the Kuroshio across the continental shelf northeast of Taiwan. J. Geophy. Res., *97*, C9, 14323–14330.

Hsueh, Y.; C.-S. Chern and J. Wang. 1993. Blocking of the Kuroshio by the Continental Shelf Northeast of Taiwan. J. Geophy. Res., *98*, C7, 12351–12359.

Jan, S.; C.-C. Chen; Y.-L. Tsai; Y. J. Yang; J. Wang; C.-S. Chern; G. Gawarkiewicz; R.-C. Lien; L. Centurioni and J.-Y. Kuo. 2011. Mean structure and variability of the Cold Dome northeast of Taiwan., Oceanography, *24*, 100–109.

Jan, S.; J. Wang; Y.-J. Yang; C.-C. Hung; C.-S. Chern; G. Gawarkiewicz; R.-C. Lien; L. Centurioni; J.-Y. Kuo and B. Wang. 2013. Observation of a freshwater pulse induced by Typhoon Morakot off the northern coast of Taiwan in August 2009. J. Mar. Res., *71*(1–2), 19–46.

Mellor, G. L. and P. A. Durbin. 1975. The structure and dynamics of the ocean surface mixed layer. J. Phys. Oceanogr., *5*, 718–728.

Morimoto, A.; S. Kojima; S. Jan and D. Takahashi. 2009. Movement of the Kuroshio axis to the northeast shslef of Taiwan during typhoon events. Estuar. Coast. Shelf Sci., *82*, 547–552.

Rudnick, D. L.; S. Jan; L. Centurioni; C. M. Lee; R.-C. Lien; J. Wang; D.-K. Lee; R.-S. Tseng; Y. Y. Kim and C.-S. Chern. 2011. Seasonal and mesoscale variability of the Kuroshio near its origin. Oceanography, *24*, 52–63.

Semtner, A. J. and Y. Mintz. 1977. Numerical simulation of the Gulf Stream and mid-ocean eddies. J. Phys. Oceanogr., *7*, 208–230.

Schloemer, R. W. 1954. Analysis and synthesis of hurricane wind patterns over Lake Okechobee, Florida. Hydromet. Rep. *31*, Dept. of Commerce, Washington, DC.

Tsai, Y.-L.; C.-S. Chern and J. Wang. 2008a. Typhoon induced upper ocean cooling off northeastern Taiwan, Geophysical Research Letters, *35*, L14605, doi:10.1029/2008GL034368.

Tsai, Y.-L.; C.-S. Chern and J. Wang. 2008b. The upper ocean response to a moving typhoon. J. of Oceanogr., *64*, 115–130.

Received: *June 27, 2012*; Revised: *Feb. 11, 2013*.